



Quantum noise spectroscopy as an incoherent imaging problem

Mankei Tsang ^{*}

Department of Electrical and Computer Engineering, National University of Singapore, 4 Engineering Drive 3, Queenstown 117583, Singapore
and Department of Physics, National University of Singapore, 2 Science Drive 3, Queenstown 117551, Singapore

 (Received 20 September 2022; revised 29 November 2022; accepted 6 January 2023; published 19 January 2023)

I point out the mathematical correspondence between an incoherent imaging model proposed by my group in the study of quantum-inspired superresolution [M. Tsang, R. Nair, and X.-M. Lu, *Phys. Rev. X* **6**, 031033 (2016)] and a noise spectroscopy model also proposed by us [M. Tsang and R. Nair, *Phys. Rev. A* **86**, 042115 (2012); S. Ng *et al.*, *ibid.* **93**, 042121 (2016)]. Both can be regarded as random displacement models, where the probability measure for the random displacement depends on unknown parameters. The spatial-mode demultiplexing (SPADE) method proposed for imaging is analogous to the spectral photon counting method proposed by Ng *et al.* for optical phase noise spectroscopy: Both methods are discrete-variable measurements that are superior to direct displacement measurements (direct imaging or homodyne detection) and can achieve the respective quantum limits. Inspired by SPADE, I propose a modification of spectral photon counting when the input field is squeezed: The output field is simply unsqueezed before spectral photon counting. I show that this method is quantum optimal and far superior to homodyne detection for both parameter estimation and detection, thus solving the open problems in the work of Tsang and Nair and Ng *et al.*

DOI: [10.1103/PhysRevA.107.012611](https://doi.org/10.1103/PhysRevA.107.012611)

I. INTRODUCTION

Optical telescopes and gravitational-wave detectors are two of the most important technologies in modern physics and astronomy. This paper studies a remarkable connection between them from the perspective of quantum metrology. The key insight is that the photons from incoherent sources received by a telescope and an optomechanical system under a stochastic gravitational-wave background can be modeled as quantum systems under random displacements, as depicted in Fig. 1. In both the imaging problem and the stochastic background sensing problem, measurements are performed to estimate the probabilistic properties of the displacements and the measurements for both problems turn out to share significant similarities in a statistical sense. My group has studied both problems [1–4], but in those works the connection was not elaborated. Inspired by the connection, here I use the insights gained from our study of incoherent imaging to devise an optimal measurement for an optical random displacement model with squeezed light, thus solving the open problems in Refs. [3,4]. The optimal measurement is far superior to the standard homodyne detection in the same way quantum-inspired imaging methods can beat direct imaging. Beyond imaging, optomechanics, and gravitational-wave detection, the random displacement model is also relevant to magnetometers under fluctuating magnetic fields [5] and microwave cavities driven by hypothetical dark-matter axions [6], so the insights and results here should have wider implications.

II. MODELS

Consider first the incoherent imaging system depicted in Fig. 1(a). The one-photon density operator ρ on the image plane can be modeled as [1,2]

$$\rho = \int dP U_X |\psi\rangle\langle\psi| U_X^\dagger, \quad (1)$$

$$U_X = \prod_{m=1}^M \exp(-ik_m X_m), \quad (2)$$

where M is the dimension of the object and image planes, $|\psi\rangle$, an element of the Hilbert space $\mathcal{H} = \mathcal{H}_1 \otimes \cdots \otimes \mathcal{H}_M$, models the diffraction-limited point-spread function of the imaging system, k_m is a momentum operator on \mathcal{H}_m , U_X is a unitary operator that models the photon displacement on the image plane due to a point source, and X is a real classical M -dimensional random vector under the probability measure P , which models the object intensity function. Mathematically, Eq. (1) is a Bochner integral; both dP and X in Eq. (1) depend implicitly on $x \in S$ in terms of a probability space (S, Σ, P) [7].

The imaging problem can be framed as a quantum detection or estimation problem [2,8], where P belongs to a family of probability measures $\{P_\theta : \theta \in \Theta\}$ parametrized by a parameter θ in some parameter space Θ and a parameter of interest $\beta(\theta)$ is to be estimated via measurements of the optical fields. Studies in the area of quantum-inspired superresolution have shown that spatial-mode demultiplexing (SPADE) can offer a far superior performance over direct imaging and achieve the quantum limits in the resolution of two point sources [1,9], object-size estimation [10,11], and moment estimation [10,12–17]. For the uninitiated, Appendixes A and B offer a brief review of these results.

^{*}mankei@nus.edu.sg; <https://blog.nus.edu.sg/mankei>.

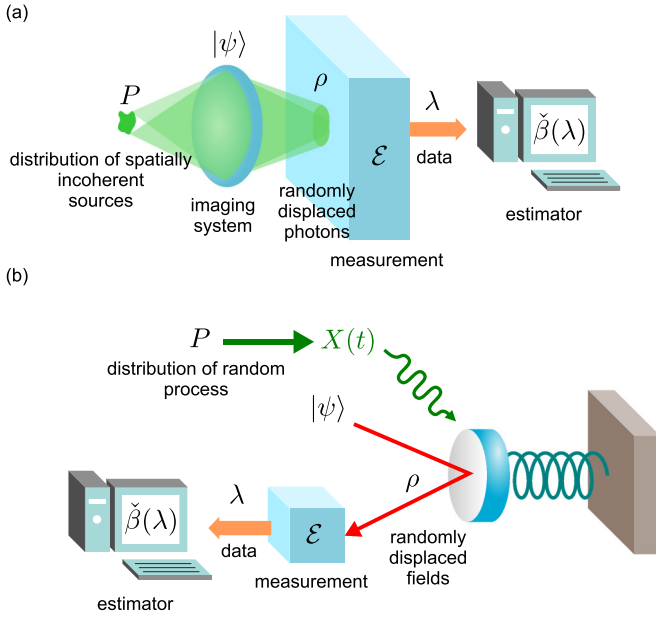


FIG. 1. (a) Schematic of an incoherent imaging system, where the quantum state ρ of each image-plane photon can be modeled as a randomly displaced object, with the distribution of the incoherent sources determining the probability measure P for the displacement and the point-spread function of the imaging system determining the initial state $|\psi\rangle$ of the photon. (b) Schematic of an optomechanical sensor, where the quantum state ρ of the optical fields before the measurement can also be modeled as a randomly displaced object, with a probability measure P governing the displacement and the initial state of the optical fields determining $|\psi\rangle$. In both cases, a measurement is modeled by a positive-operator-valued measure \mathcal{E} , and an estimator $\hat{\beta}(\lambda)$ of a parameter of P can be constructed from the measurement outcome λ .

The incoherent imaging model turns out to be mathematically similar to a noise spectroscopy model also proposed by my group in Refs. [3,4]. The main difference is in the dimension M : Imaging problems usually assume that M is 1 or 2, whereas Refs. [3,4] assume that it is infinite. In the noise spectroscopy problem, ρ is the state of a quantum dynamical system coupled to quantum fields, $|\psi\rangle$ is an element of an infinite-dimensional Hilbert space \mathcal{H} that models the input state of the total system, $X(t)$ is a real classical random process with respect to a time variable t that generalizes the m in Eq. (2), and the unitary is

$$U_X = \mathcal{T} \exp \left(-i \int_0^T dt k(t) X(t) \right), \quad (3)$$

where \mathcal{T} denotes time ordering, T is the total observation time, and $k(t)$ is a Hermitian operator on \mathcal{H} in an interaction picture [18]. Further, $|\psi\rangle$ and $k(t)$ are assumed to be independent of X . Any sequential measurements concurrent with the displacement can be modeled as a final measurement via the principle of deferred measurement [19,20]. Examples include an optical field under a random displacement or phase modulation, an optomechanical system under a stochastic force [21,22], a gravitational-wave detector under a stochastic background [23], a spin ensemble under a stochastic magnetic field

[5], and a microwave cavity driven by dark-matter axions [6]. Figure 1(b) depicts an optomechanical system as an example.

References [3,4] assume that $X(t)$ is a stationary zero-mean Gaussian random process and its power spectral density $S_X(\omega|\theta)$ depends on the unknown parameter θ . Reference [3] assumes that Θ is binary with $S_X(\omega) = 0$ for one of the hypotheses, such that the problem of interest is the detection of a random displacement, while Ref. [4] assumes that Θ is a multidimensional Euclidean space, such that the problem is spectrum-parameter estimation. In other words, Refs. [3,4] assume parametric models for the probability measure P , in the same way parametric models for P are assumed for incoherent imaging.

III. SPECTRUM-PARAMETER ESTIMATION

The power spectral density, being a second-order statistic, is analogous to the second-order object moments in the context of imaging. Since SPADE can enhance the estimation of second-order moments [10,12–17], it is natural to ask if a similar enhancement can be found for noise spectroscopy. The answer is yes: Ref. [4] considers an optical field under weak and random phase modulation and finds that spectral photon counting, a discrete-variable measurement analogous to SPADE, can be far superior to homodyne detection, a continuous-variable measurement analogous to direct imaging, when the input state $|\psi\rangle$ is a coherent state. Spectral photon counting is quantum optimal and enjoys significant superiority over homodyne detection in the regime of low signal-to-noise ratios, just as SPADE is quantum optimal and superior in the regime of subdiffraction object sizes for imaging.

In the following, I adopt a level of mathematical rigor typical of the physics and engineering literature [24,25] to arrive at results quickly, following Refs. [3,4]. To derive a quantum limit to noise spectroscopy, Ref. [4] makes the following assumptions.

Assumption 1. $X(t)$ is a zero-mean Gaussian process.

Assumption 2. The processes $X(t)$ and

$$\Delta k(t) \equiv k(t) - \langle \psi | k(t) | \psi \rangle \quad (4)$$

are stationary in the wide sense [24,26,27] such that

$$C_X(\tau|\theta) \equiv \mathbb{E}_\theta[X(t)X(t+\tau)], \quad (5)$$

$$C_k(\tau) \equiv \langle \psi | \Delta k(t) \circ \Delta k(t+\tau) | \psi \rangle \quad (6)$$

are independent of t . [\mathbb{E}_θ denotes the expectation with respect to P_θ and $A \circ B \equiv (AB + BA)/2$ denotes the Jordan product.]

Assumption 3. The observation time T is long enough to justify certain approximations regarding stationary processes [26,27].

Such assumptions are common in statistics [26,27] and have the virtue of giving simple closed-form results for the infinite-dimensional model. Assuming also that θ is a real scalar for simplicity, a quantum limit to the Fisher information J for any measurement is [4]

$$J \leq K \leq \tilde{K} \rightarrow T \int_{-\infty}^{\infty} \frac{d\omega}{2\pi} \frac{(\partial \ln S_X)^2}{2 + 1/S_k S_X}, \quad (7)$$

$$S_X(\omega|\theta) \equiv \int_{-\infty}^{\infty} d\tau C_X(\tau|\theta) \exp(i\omega\tau), \quad (8)$$

$$S_k(\omega) \equiv \int_{-\infty}^{\infty} d\tau C_k(\tau) \exp(i\omega\tau), \quad (9)$$

where K is the Helstrom information in terms of ρ as a function of θ [8,28], \tilde{K} is a bound derived in Ref. [4] using the extended convexity of K [29], $\partial \equiv \partial/\partial\theta$, and \rightarrow denotes the long-time limit. These information quantities determine the fundamental limits to the estimation of a parameter θ of the power spectral density $S_X(\omega|\theta)$ of the “noise” $X(t)$ in noise spectroscopy. For the uninitiated, Appendixes A and C give a brief review of the basic concepts in quantum estimation theory.

Note that Eq. (7) is applicable to scenarios where the probe is initially entangled with an ancilla, as $|\psi\rangle$ can model the initial state of the probe plus the ancilla in a larger Hilbert space and U_X can be an operator on the probe subspace only.

At the time of Ref. [4], we were unable to find a quantum-optimal measurement when the input state is not a coherent state, but the correspondence with incoherent imaging offers a new insight. We know that SPADE can remain superior and optimal as long as its basis is adapted to $|\psi\rangle$ [1,9,12,16,30]. This fact suggests that a discrete-variable measurement is still optimal for noise spectroscopy with a nonclassical state, as long as the measurement basis is adapted to the input state $|\psi\rangle$. If $|\psi\rangle$ is a squeezed state, it still has a Gaussian wave function and is analogous to a Gaussian point-spread function in imaging. The imaging correspondence then suggests that an optimal basis adapted to $|\psi\rangle$ is simply a squeezed version of an optimal basis adapted to the vacuum. A measurement in that basis can be implemented by unsqueezing the output field, analogous to an image magnification, before spectral photon counting.

I now show the optimality of the unsqueezing and spectral photon counting (USPC) method in detail. Let

$$k(t) = A^\dagger(t)A(t), \quad [A(t), A^\dagger(t')] = \delta(t - t'), \quad (10)$$

where $A(t)$ is the annihilation operator for the slowly varying envelope of an optical field with carrier frequency Ω [24,25] and $k(t)$ is the photon-flux operator. Then X is a phase modulation on the optical field. Since $k(t)$ commutes with itself at different times, the time ordering in Eq. (3) is redundant. Assume also that

$$|\psi\rangle = D(\alpha)V|\text{vac}\rangle, \quad (11)$$

where $|\text{vac}\rangle$ is the vacuum state, V is a unitary operator that models the squeezing, and $D(\alpha)$ is the displacement operator that gives a constant mean field $\langle\psi|A(t)|\psi\rangle = \alpha$. Note that $|\alpha|^2$ is the mean photon flux. With a high $|\alpha|$ and weak phase modulation, $D^\dagger k(t)D$ can be linearized as an intensity quadrature operator

$$D^\dagger k(t)D \approx |\alpha|^2 + \kappa(t), \quad \kappa(t) \equiv \alpha A^\dagger(t) + \alpha^* A(t), \quad (12)$$

and $D^\dagger U_X D$ becomes a displacement operator. This linearization turns the phase modulation into a displacement. The initial squeezing V should squeeze the orthogonal phase

quadrature

$$\eta(t) \equiv \frac{1}{2i|\alpha|^2} [\alpha A^\dagger(t) - \alpha^* A(t)] \quad (13)$$

and antisqueeze the intensity quadrature such that

$$V^\dagger \eta V = h * \eta, \quad V^\dagger \kappa V = g * \kappa, \quad (14)$$

where $h * \eta \equiv \int_{-\infty}^{\infty} dt' h(t - t') \eta(t')$ denotes the convolution and the real Green's functions $h(t)$ and $g(t)$ model the squeezing and the antisqueezing, respectively [24]. Their Fourier transforms are related by

$$|\tilde{h}(\omega)\tilde{g}(\omega)| = 1, \quad (15)$$

where

$$\tilde{g}(\omega) \equiv \int_{-\infty}^{\infty} dt g(t) \exp(i\omega t), \quad (16)$$

and $\tilde{h}(\omega)$ is defined similarly.

After U_X , suppose that the mean field is nulled by $D^\dagger(\alpha)$ and then the squeezing is undone by a unitary W , which is the same as V except that a negative sign is introduced to the parametric-amplifier Hamiltonian. In other words, the experimental setup for the unsqueezing can be the same as that for V , except that the phase of the pump beam should be shifted by π if the parametric amplifier is implemented by three-wave mixing. The effect of W on the quadratures can be modeled as

$$W^\dagger \eta W = g * \eta, \quad W^\dagger \kappa W = h * \kappa. \quad (17)$$

Note that W is not V^\dagger , as the Green functions would become anticausal and thus unphysical if W were V^\dagger . Conditioned on X , the output state

$$|\psi'\rangle = W D^\dagger U_X D V |\text{vac}\rangle \quad (18)$$

is a coherent state with mean field

$$\alpha'(t) \equiv \langle\psi'|A(t)|\psi'\rangle = -i\alpha g * X, \quad (19)$$

where the displacement in the phase quadrature is amplified by the unsqueezing. This model is also applicable to the dark port of a Michelson interferometer [31], where the squeezing V and the unsqueezing W should be applied to the input and output of the dark port, respectively, the displacements D and D^\dagger are naturally implemented by a strong beam at the other input port and the beam splitter in the interferometer, and X is proportional to the relative phase between the two arms, as depicted by Fig. 2. Any radiation-pressure-induced noise is assumed to be negligible or eliminated [32,33].

To facilitate the analysis of the subsequent step of spectral photon counting, I discretize frequency by assuming that $X(t)$ is given by the Fourier series

$$X(t) = \frac{1}{\sqrt{T}} \sum_{m=-\infty}^{\infty} \tilde{X}_m \exp(-i\omega_m t), \quad \omega_m \equiv \frac{2\pi m}{T}, \quad (20)$$

$$\tilde{X}_m \equiv \frac{1}{\sqrt{T}} \int_0^T dt X(t) \exp(i\omega_m t). \quad (21)$$

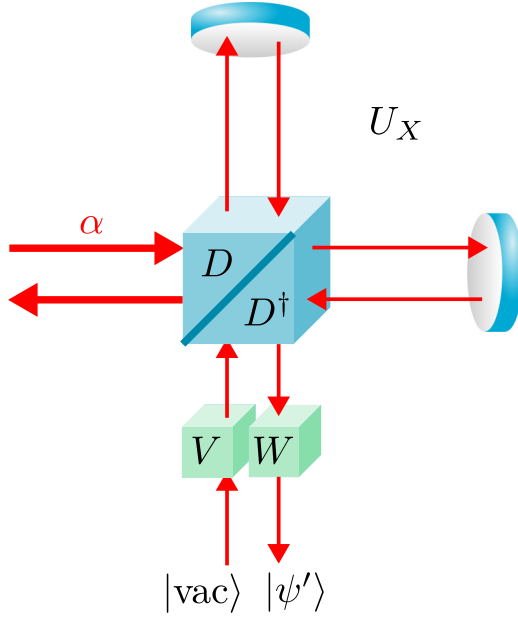


FIG. 2. Michelson implementation of the model given by Eqs. (11)–(19).

Then the mean field of the output coherent state given by Eq. (19) can be expressed as

$$\alpha'(t) = -\frac{i\alpha}{\sqrt{T}} \sum_{m=-\infty}^{\infty} \tilde{g}(\omega_m) \tilde{X}_m \exp(-i\omega_m t). \quad (22)$$

Suppose that a spectrometer disperses the output field in terms of frequency modes defined by the annihilation operators

$$a_m \equiv \frac{1}{\sqrt{T}} \int_0^T dt A(t) \exp(i\omega_m t), \quad m \in \mathbb{Z}, \quad (23)$$

where ω_m is a sideband frequency relative to the carrier Ω [34]. Each frequency mode is then in a coherent state with a displacement given by

$$\tilde{\alpha}_m \equiv \langle \psi' | a_m | \psi' \rangle = \alpha \tilde{g}(\omega_m) \tilde{X}_m. \quad (24)$$

Since $X(t)$ is real, $\tilde{X}_{-m} = \tilde{X}_m^*$. Assume that $\{\tilde{X}_m : m > 0\}$ are independent zero-mean complex Gaussian random variables, each with variance

$$\mathbb{E}_\theta(|\tilde{X}_m|^2) = S_X(\omega_m|\theta). \quad (25)$$

Assume also that \tilde{X}_0 is a zero-mean real Gaussian random variable that is independent of the rest. These assumptions allow the Fourier series given by Eq. (20) to approach any real stationary zero-mean Gaussian process in the long-time limit [27]. By summing the photon counts at each pair of sideband frequencies $-\omega_m$ and ω_m , one obtains a set of photon counts that follow the Bose-Einstein distribution

$$f_\theta(n) = \prod_{m>0} \frac{1}{1 + \bar{N}_m} \left(\frac{\bar{N}_m}{1 + \bar{N}_m} \right)^{n_m}, \quad (26)$$

$$\bar{N}_m(\theta) = 2\mathbb{E}_\theta(|\tilde{\alpha}_m|^2) = 2|\alpha \tilde{g}(\omega_m)|^2 S_X(\omega_m|\theta). \quad (27)$$

The $m = 0$ mode has a more complicated photon counting distribution that need not be considered, as there is a continuum

of modes in the long-time limit and the information provided by one mode should be negligible. The Fisher information for USPC is hence

$$J_{\text{USPC}} \equiv \sum_n f_\theta(n) [\partial \ln f_\theta(n)]^2 \quad (28)$$

$$= \sum_{m>0} \frac{(\partial \ln \bar{N}_m)^2}{1 + 1/\bar{N}_m} \quad (29)$$

$$\rightarrow T \int_{-\infty}^{\infty} \frac{d\omega}{2\pi} \frac{(\partial \ln S_X)^2}{2 + 1/|\alpha \tilde{g}|^2 S_X}, \quad (30)$$

where the long-time limit gives $\sum_{m>0} \rightarrow T \int_0^\infty d\omega/2\pi$ and the integral $\int_0^\infty d\omega$ for an even integrand is rewritten as the double-sided integral $\int_{-\infty}^\infty d\omega/2$ for easier comparison with Eq. (7).

To compare this result with the quantum bound, note that the power spectral density of $\Delta k(t)$ with respect to $|\psi\rangle = DV|\text{vac}\rangle$ is the same as that of $\Delta k'(t)$ with respect to $|\text{vac}\rangle$, where $k'(t) \equiv V^\dagger D^\dagger k(t) DV$, and the antisqueezing of the intensity quadrature by V leads to

$$S_k(\omega) = |\alpha \tilde{g}(\omega)|^2. \quad (31)$$

With this $S_k(\omega)$, the USPC information given by Eq. (30) matches the quantum bound \tilde{K} given by Eq. (7) and is hence quantum optimal.

For comparison, the Fisher information for homodyne detection of the phase quadrature $U_X^\dagger \eta U_X = \eta + X$ is [4,35]

$$J_{\text{hom}} \rightarrow T \int_{-\infty}^{\infty} \frac{d\omega}{2\pi} \frac{(\partial \ln S_X)^2}{2 + 4S_\eta/S_X + 2(S_\eta/S_X)^2}, \quad (32)$$

where η is assumed to be a stationary zero-mean Gaussian process with power spectral density S_η . For the squeezed $|\psi\rangle$,

$$S_\eta(\omega) = \frac{1}{4S_k(\omega)}, \quad (33)$$

and $S_\eta S_k \geq \frac{1}{4}$ in general [24]. Compared with the optimal information given by Eqs. (7) and (30), the homodyne information with a quantum-limited S_η has an extra factor $2(S_\eta/S_X)^2$ in the denominator, which is significant when the spectral signal-to-noise ratio (SNR) S_X/S_η is low. To see their difference more clearly, assume that

$$\frac{S_X}{S_\eta} = 4S_k S_X \ll 1 \quad (34)$$

and perform Taylor approximations of Eqs. (7), (30), and (32), which give

$$J_{\text{USPC}} \approx \tilde{K} \approx T \int_{-\infty}^{\infty} \frac{d\omega}{2\pi} S_k S_X (\partial \ln S_X)^2, \quad (35)$$

$$J_{\text{hom}} \approx 8T \int_{-\infty}^{\infty} \frac{d\omega}{2\pi} (S_k S_X)^2 (\partial \ln S_X)^2. \quad (36)$$

The J_{hom} is much lower because of an extra factor of $8S_k S_X$ in the integrand.

For a simple example, suppose that $S_X(\omega|\theta) = \theta^2 R(\omega)$, where θ is the magnitude of the displacement and $R(\omega)$ is a known spectrum. In other words, the shape of the noise spectrum is assumed to be known and one is simply interested

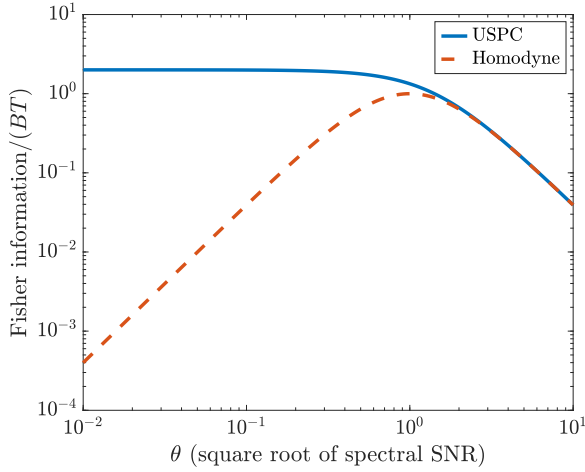


FIG. 3. Comparison of USPC and homodyne detection in terms of their Fisher information given by Eqs. (42) as a function of θ in log-log scale. The Fisher information has been normalized with respect to the time-bandwidth product BT . The θ has been normalized so that θ^2 is the ratio of the displacement spectrum S_X to the quantum-limited phase-quadrature spectrum $S_\eta = 1/4S_k$. Both axes are dimensionless.

in estimating the height of $\sqrt{S_X(\omega|\theta)}$. Then

$$J_{\text{USPC}} \approx \tilde{K} \rightarrow T \int_{-\infty}^{\infty} \frac{d\omega}{2\pi} \frac{4}{2\theta^2 + 1/S_k R}, \quad (37)$$

$$J_{\text{hom}} \rightarrow T \int_{-\infty}^{\infty} \frac{d\omega}{2\pi} \frac{4}{2\theta^2 + 1/S_k R + 1/8(\theta S_k R)^2}. \quad (38)$$

As $\theta \rightarrow 0$, J_{hom} scales quadratically with θ and vanishes, while J_{USPC} tends to a positive constant. These behaviors are analogous to the phenomenon of Rayleigh's curse for direct imaging and the superiority of SPADE in two-point resolution and object-size estimation [1,10,11].

To be even more concrete, suppose that both $S_k(\omega) = |\alpha \tilde{g}(\omega)|^2$ and $R(\omega)$ are flat within the band $|\omega| \leq 2\pi B$ and $R(\omega) = 0$ otherwise. Furthermore, assume an $R(0)$ so that θ^2 is the spectral SNR. In other words, assume that

$$S_k(\omega) = S_k(0) \text{ if } |\omega| \leq 2\pi B, \quad (39)$$

$$R(\omega) = \begin{cases} S_\eta(0) = 1/4S_k(0) & \text{for } |\omega| \leq 2\pi B \\ 0 & \text{otherwise,} \end{cases} \quad (40)$$

$$\theta^2 = \frac{S_X(0|\theta)}{S_\eta(0)} = 4S_k(0)S_X(0|\theta). \quad (41)$$

Then

$$J_{\text{USPC}} \rightarrow \frac{4BT}{\theta^2 + 2}, \quad J_{\text{hom}} \rightarrow \frac{4BT}{\theta^2 + 2 + 1/\theta^2}, \quad (42)$$

which are plotted in log-log scale in Fig. 3. Notice the difference in the scalings for $\theta \ll 1$ and the substantial widening gap.

In practice, the unknown parameter of the noise spectrum is of course often multidimensional or even the function S_X itself with no simple parametric model. The results on multiparameter or semiparametric estimation in imaging offer

encouragement that the superiority of USPC should still persist for those more complicated problems.

IV. STOCHASTIC-DISPLACEMENT DETECTION

Consider now the detection problem studied in Ref. [3]. Let $\theta \in \Theta = \{0, 1\}$, P_0 be the measure that gives the deterministic $X = 0$ when the displacement is absent, P_1 be the measure for X when the displacement is present, and ρ_θ be the quantum state as a function of θ . Since $\rho_0 = |\psi\rangle\langle\psi|$ is pure in this problem, the Uhlmann fidelity is given by

$$F \equiv \text{tr} \sqrt{\sqrt{\rho_0} \rho_1 \sqrt{\rho_0}} = \sqrt{\langle \psi | \rho_1 | \psi \rangle}, \quad (43)$$

while the quantum Chernoff exponent ζ [36] is given by

$$\xi \leq \zeta \equiv -\ln \inf_{0 \leq s \leq 1} \text{tr}(\rho_0^{1-s} \rho_1^s) = -2 \ln F, \quad (44)$$

where ξ is the classical Chernoff exponent for any measurement. F and ζ can be used to set a variety of lower and upper bounds on the error probabilities under the Bayesian or Neyman-Pearson criterion; see Appendix D for a quick summary of the Bayesian theory.

In addition to Assumptions 1–3 for P_1 and $|\psi\rangle$, assume also the following.

Assumption 4. The initial state $|\psi\rangle$ is a Gaussian state.

Assumption 5. The Hermitian operator $k(t)$ is a linear function of bosonic creation and annihilation operators such that U_X is a displacement operator.

The quantum exponent is then given by [3]

$$\zeta \rightarrow \frac{T}{2} \int_{-\infty}^{\infty} \frac{d\omega}{2\pi} \ln(1 + 2S_k S_X). \quad (45)$$

We also considered in Ref. [3] the performances of the Kennedy receiver and the homodyne detection for the optical model, but we were unable to find the exact optimal measurement at the time. Here I solve the open problem by showing that USPC is also optimal for the detection problem, in analogy with the optimality of SPADE for the binary-source detection problem [9]. Assuming again weak phase modulation, the USPC distribution given by Eqs. (26) and (27), and

$$S_X(\omega|0) = 0, \quad f_0(n) = \delta_{n0}, \quad S_X(\omega|1) = S_X(\omega), \quad (46)$$

the Chernoff exponent is

$$\xi_{\text{USPC}} \equiv -\ln \inf_{0 \leq s \leq 1} \sum_n [f_0(n)]^{1-s} [f_1(n)]^s \quad (47)$$

$$= \sum_{m>0} \ln[1 + \bar{N}_m(1)] \quad (48)$$

$$\rightarrow \frac{T}{2} \int_{-\infty}^{\infty} \frac{d\omega}{2\pi} \ln(1 + 2|\alpha \tilde{g}|^2 S_X). \quad (49)$$

With the S_k given by Eq. (31), ξ_{USPC} matches the quantum limit ζ given by Eq. (45).

For comparison, consider the classical Chernoff exponent for homodyne detection given by [3,27]

$$\xi_{\text{hom}} \rightarrow \sup_{0 \leq s \leq 1} \frac{T}{2} \int_{-\infty}^{\infty} \frac{d\omega}{2\pi} \ln \left(\frac{1 + (1-s)S_X/S_\eta}{(1 + S_X/S_\eta)^{1-s}} \right). \quad (50)$$

The imaging correspondence suggests that there should be a significant gap between ζ and ξ_{hom} , although we did not

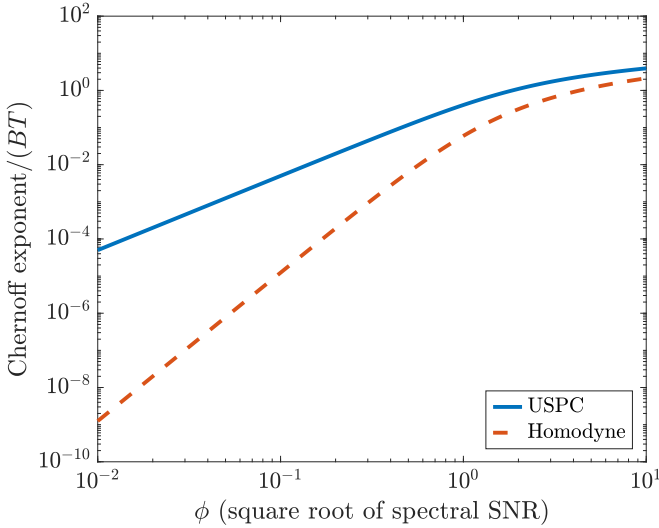


FIG. 4. Comparison of USPC and homodyne detection in terms of their Chernoff exponents given by Eqs. (49) and (50), assuming the flat spectra given by Eqs. (39) and (40). The horizontal axis ϕ is the square root of the spectral SNR defined by Eq. (54). The Chernoff exponent has been normalized with respect to the time-bandwidth product BT . The plot is in log-log scale and both axes are dimensionless.

realize it at the time of Ref. [3]. To demonstrate the gap now, assume again a low spectral SNR as per Eq. (34) and perform Taylor approximations of Eqs. (45), (49), and (50), which give

$$\xi_{\text{USPC}} \approx \zeta \approx T \int_{-\infty}^{\infty} \frac{d\omega}{2\pi} S_k S_X, \quad (51)$$

$$\xi_{\text{hom}} \approx \sup_s \frac{s(1-s)T}{4} \int_{-\infty}^{\infty} \frac{d\omega}{2\pi} \left(\frac{S_X}{S_\eta} \right)^2 \quad (52)$$

$$= T \int_{-\infty}^{\infty} \frac{d\omega}{2\pi} (S_k S_X)^2. \quad (53)$$

The optimal exponent is linear with respect to S_X , whereas the homodyne exponent is only quadratic. These scalings are analogous to the scalings of the optimal exponent and the direct-imaging exponent with respect to the source separation in the binary-source detection problem [9].

For a more concrete example, assume the flat spectra given by Eqs. (39) and (40) and define

$$S_X(\omega) = \phi^2 R(\omega) \quad (54)$$

so that the spectral SNR is now ϕ^2 and ϕ plays the same role as θ in Fig. 3. Figure 4 plots the resulting Chernoff exponents given by Eqs. (49) and (50) against ϕ in log-log scale.

It is possible to study the error probabilities of the detection problem more precisely under the Neyman-Pearson criterion [3,28,37,38], although the insights offered by such calculations should not deviate much from the ones reported here.

V. DISCUSSION

Since homodyne detection is the current standard measurement method in gravitational-wave detection [39], the superior scalings of the USPC information quantities indicated by

Eqs. (35), (36), (51), and (53) are important discoveries. They suggest that USPC can substantially enhance the detection and spectroscopy of stochastic gravitational-wave backgrounds when the spectral SNR is low, in the same way SPADE can enhance incoherent imaging. Considering that squeezed light is now being used in gravitational-wave detectors [40], the unsqueezing step proposed here is important, as it optimizes the measurement for squeezed light beyond the coherent-state case considered in Refs. [3,4] and allows the full potential of quantum-enhanced interferometry to be realized for noise spectroscopy.

A potential practical issue with the proposal is its assumption of quantum-limited squeezing and unsqueezing in both quadratures. Optical squeezers in current technology often introduce excess noise in the antisqueezed quadrature, which has little impact on the homodyne detection of the squeezed quadrature but may add significant noise to the photon counting step here. With two squeezers in the proposed setup, the issue of excess noise is even worse. In view of the amazing achievements of the experimentalists in LIGO and squeezing, however, one should never underestimate their skills, and the superiority of USPC should motivate the current and future generations to reach even greater heights in squeezing technology in order to achieve the promised improvement.

The correspondence between the incoherent imaging model and the random displacement model is used implicitly in Sec. 6 of Ref. [10] and briefly mentioned in Ref. [13] but not elaborated there. References [41,42] point out the correspondence between incoherent imaging and noise spectroscopy more explicitly, although they assume a low dimension for the Hilbert space and somewhat different parametric models. A more recent outstanding work by Górecki *et al.* [43] also notices the correspondence and also uses the convexity of the Helstrom information to derive a quantum bound for a random displacement model with one optical mode. They discovered independently that unsqueezing before photon counting is optimal for a squeezed input state and superior to homodyne detection. Another outstanding relevant work is Ref. [44] by Shi and Zhuang, who also discovered independently the optimality and superiority of unsqueezing and photon counting for a somewhat different random displacement model, which can be obtained by applying a rotating-wave approximation to the unitary given by Eq. (3) and imposing a thermal channel. References [41–44] all do not consider the detection problem and are not aware of the prior Refs. [3,4].

As there exist many other results in quantum-inspired superresolution that have not yet been translated to noise spectroscopy, and vice versa, the correspondence between the two models should have much more to give.

ACKNOWLEDGMENTS

This research is supported by the National Research Foundation, Singapore, under its Quantum Engineering Programme (QEP-P7).

APPENDIX A: QUANTUM ESTIMATION THEORY

Let $\{\rho_\theta : \theta \in \Theta\}$ be a family of density operators. Given a parameter θ and after a measurement modeled by a positive-

operator-valued measure (POVM) \mathcal{E} , the probability measure Q_θ for the measurement outcome λ being in a set A is given by [7]

$$Q_\theta(A) = \text{tr} \mathcal{E}(A) \rho_\theta, \quad (\text{A1})$$

where tr is the operator trace. Let the parameter of interest be a real scalar $\beta(\theta)$ and an estimator be $\check{\beta}(\lambda)$. The mean-square error is defined as

$$\text{MSE}(\theta) \equiv \mathbb{E}_\theta \{ [\check{\beta} - \beta(\theta)]^2 \} \quad (\text{A2})$$

$$= \int dQ_\theta(\lambda) [\check{\beta}(\lambda) - \beta(\theta)]^2, \quad (\text{A3})$$

where \mathbb{E}_θ denotes the expectation given θ . Let θ be a real scalar and suppose that each Q_θ possesses a probability density $f_\theta(\lambda)$ with respect to a θ -independent reference measure ν . Assuming the local unbiased condition for the estimator given by

$$\mathbb{E}_\theta(\check{\beta}) = \beta(\theta), \quad (\text{A4})$$

$$\int d\nu(\lambda) \check{\beta}(\lambda) \partial f_\theta(\lambda) = \mathbb{E}_\theta(\check{\beta} \partial \ln f_\theta) = \partial \beta(\theta), \quad (\text{A5})$$

$$\partial \equiv \frac{\partial}{\partial \theta}, \quad (\text{A6})$$

the classical Cramér-Rao bound is

$$\text{MSE}(\theta) \geq \frac{[\partial \beta(\theta)]^2}{J(\theta)}, \quad J(\theta) \equiv \mathbb{E}_\theta [(\partial \ln f_\theta)^2], \quad (\text{A7})$$

where $J(\theta)$ is called the Fisher information. The bound is also achievable with the maximum-likelihood estimator in an asymptotic sense and can be generalized for more relaxed conditions [26].

A quantum bound on J for any POVM \mathcal{E} is [28]

$$J(\theta) \leq K(\theta) \equiv \text{tr} \rho_\theta L_\theta^2, \quad (\text{A8})$$

where $K(\theta)$ is the Helstrom information [8], L_θ is a solution to

$$\partial \rho_\theta = \rho_\theta \circ L_\theta, \quad (\text{A9})$$

and \circ denotes the Jordan product of two operators defined as

$$A \circ B \equiv \frac{1}{2}(AB + BA). \quad (\text{A10})$$

Generalization of these results for a multidimensional parameter can be done by considering the matrix versions of the information quantities [28] or adopting the parametric-submodel approach [16,45,46].

APPENDIX B: QUANTUM-INSPIRED SUPERRESOLUTION

Consider the incoherent imaging model given by Eqs. (1) and (2) in one dimension ($M = 1$). For the estimation of the separation between two point sources, the probability measure P_θ as a function of the separation $\theta \in \mathbb{R}$ can be modeled as

$$P_\theta = \frac{1}{2}(\delta_{-\theta/2} + \delta_{\theta/2}), \quad (\text{B1})$$

where

$$\delta_x(A) \equiv \begin{cases} 1 & \text{for } x \in A \\ 0 & \text{otherwise} \end{cases} \quad (\text{B2})$$

is the Dirac measure for a unit point mass at position x . With direct imaging, which can be modeled as a measurement of the continuous photon position, the Fisher information $J(\theta)$ is roughly constant for large θ relative to Rayleigh's criterion, but it decreases when θ becomes sub-Rayleigh and drops to zero when $\theta = 0$. To distinguish this soft penalty to the Fisher information from the more heuristic Rayleigh's criterion, Ref. [1] calls the penalty Rayleigh's curse.

Unlike the direct-imaging Fisher information under Rayleigh's curse, the Helstrom information $K(\theta)$ for this problem is constant regardless of θ , meaning that the ultimate information in the photons is substantially higher than the direct-imaging information for sub-Rayleigh separations. Moreover, a measurement in the discrete Hermite-Gaussian basis called SPADE has Fisher information that coincides with the Helstrom information for all θ , meaning that SPADE is an optimal measurement and can be far superior to direct imaging for sub-Rayleigh separations [1].

A similar scenario plays out when one attempts to estimate the size of an object, for which the probability density of P_θ can be expressed as

$$\frac{dP_\theta}{dX} = \frac{1}{\theta} w\left(\frac{X}{\theta}\right) \quad (\text{B3})$$

in terms of a known function w [10,11]. For this problem, Rayleigh's curse can also be observed in the direct-imaging information, while the Helstrom information and the SPADE information approach a nonzero constant for sub-Rayleigh separations.

References [10,12–17] study the moment estimation problem, assuming that $\theta = P$ and Θ is the set of all probability measures, while the parameter of interest is

$$\beta(P) = \int dP(X) b(X), \quad (\text{B4})$$

such as the second moment with $b(X) = X^2$. As the parameter space is now infinite dimensional, the theory becomes much more formidable. However, with some effort, it can still be shown that SPADE enjoys significant superiority over direct imaging for sub-Rayleigh object sizes and is close to quantum optimal.

APPENDIX C: EXTENDED CONVEXITY

As the Helstrom information $K(\theta)$ is often difficult to compute, especially if the density operators are mixed, one may have to settle for looser bounds. If the density operator can be expressed as the mixture

$$\rho_\theta = \int dP_\theta(Z) \sigma_\theta(Z), \quad (\text{C1})$$

where $\sigma_\theta(Z)$ is a density operator conditioned on the random element Z , then a useful bound on $K(\theta)$ called the extended convexity is [4,29]

$$K(\theta) \leq \tilde{K}(\theta) \equiv \int dP_\theta(Z) K[\sigma_\theta(Z)] + J[P_\theta], \quad (\text{C2})$$

where $K[\sigma_\theta(Z)]$ is the Helstrom information in terms of $\sigma_\theta(Z)$ and $J[P_\theta]$ is the Fisher information in terms of P_θ .

To offer some intuition about the use of the extended-convexity bound in Ref. [4], consider the model given by

Eqs. (1) and (2) in one dimension ($M = 1$) for simplicity. Let

$$dP_\theta = \frac{1}{\sqrt{2\pi v_X(\theta)}} \exp\left(-\frac{X^2}{2v_X(\theta)}\right) dX \quad (\text{C3})$$

such that the variance $v_X(\theta)$ of the displacement X depends on the unknown parameter. A trick to derive a good bound is to change the random variable to $Z = X/\gamma(\theta)$ in terms of a judiciously chosen function $\gamma(\theta)$ such that

$$dP_\theta = \frac{\gamma(\theta)}{\sqrt{2\pi v_X(\theta)}} \exp\left(-\frac{\gamma(\theta)^2 Z^2}{2v_X(\theta)}\right) dZ, \quad (\text{C4})$$

$$\sigma_\theta(Z) = U_{\gamma(\theta)Z} |\psi\rangle\langle\psi| U_{\gamma(\theta)Z}^\dagger. \quad (\text{C5})$$

These expressions lead to

$$K[\sigma_\theta(Z)] = 4v_k(\partial\gamma)^2 Z^2, \quad (\text{C6})$$

$$v_k \equiv \langle\psi|k^2|\psi\rangle - (\langle\psi|k|\psi\rangle)^2, \quad (\text{C7})$$

$$\int dP_\theta(Z) K[\sigma_\theta(Z)] = 4v_k v_X (\partial \ln \gamma)^2, \quad (\text{C8})$$

$$J[P_\theta] = \frac{1}{2} \left[\partial \ln \left(\frac{v_X}{\gamma^2} \right) \right]^2, \quad (\text{C9})$$

$$\tilde{K}(\theta) = 4v_k v_X (\partial \ln \gamma)^2 + \frac{1}{2} (\partial \ln v_X - 2\partial \ln \gamma)^2, \quad (\text{C10})$$

where Eq. (C8) assumes that v_k and γ do not depend on the random variable. Picking

$$\partial \ln \gamma = \frac{\partial \ln v_X}{2 + 4v_k v_X} \quad (\text{C11})$$

hence leads to

$$\tilde{K}(\theta) = \frac{(\partial \ln v_X)^2}{2 + 1/v_k v_X}, \quad (\text{C12})$$

which resembles Eq. (7). The derivation of Eq. (7) in Ref. [4] indeed follows a similar procedure.

If P_θ is not Gaussian, a bound may still be obtained by using the convexity of the Helstrom information; Sec. 6 of Ref. [10] uses the convexity to derive a quantum limit to object-size estimation in the context of imaging and shows that SPADE can approach the limit. The trick is to change the variable in Eq. (B3) to $Z = X/\theta$, leading to

$$\rho_\theta = \int dZ w(Z) \sigma_\theta(Z), \quad \sigma_\theta(Z) = U_{\theta Z} |\psi\rangle\langle\psi| U_{\theta Z}^\dagger. \quad (\text{C13})$$

As $w(Z)$ no longer depends on θ , Eq. (C2) gives the convexity bound

$$\tilde{K}(\theta) = \int dZ w(Z) K[\sigma_\theta(Z)] = 4v_k \int dZ w(Z) Z^2, \quad (\text{C14})$$

which is independent of θ . It turns out that SPADE can achieve this bound in the limit of $\theta \rightarrow 0$ [10]. Reference [43] has obtained similar results.

APPENDIX D: QUANTUM DETECTION THEORY

Assume two hypotheses $\Theta = \{0, 1\}$. Let A be the set of measurement outcomes with which one decides on $\theta = 0$ and A^c be the set with which one decides on $\theta = 1$. Then the type-I and type-II error probabilities are, respectively,

$$Q_0(A^c) = \text{tr} \mathcal{E}(A^c) \rho_0, \quad Q_1(A) = \text{tr} \mathcal{E}(A) \rho_1. \quad (\text{D1})$$

Let π_θ be the prior probability of the hypothesis θ . Then the average error probability is

$$P_e \equiv \pi_0 Q_0(A^c) + \pi_1 Q_1(A). \quad (\text{D2})$$

Given a measurement, the classical detection problem is to choose a set A that minimizes the error probabilities. In particular, P_e can be minimized by a likelihood-ratio test [26]. Denote this minimum P_e by $P_{e,\min}$ and assume $\pi_0 = \pi_1 = \frac{1}{2}$ for simplicity. A useful lower bound on $P_{e,\min}$ is [47]

$$P_e \geq P_{e,\min} \geq \frac{1}{2} (1 - \sqrt{1 - B^2}), \quad (\text{D3})$$

where

$$B \equiv \int d\nu(\lambda) \sqrt{f_0(\lambda) f_1(\lambda)} \quad (\text{D4})$$

is the Bhattacharyya coefficient. Another useful bound is the Chernoff bound given by [26]

$$P_{e,\min} \leq \frac{1}{2} \exp(-\xi), \quad (\text{D5})$$

$$\xi \equiv -\ln \inf_{0 \leq s \leq 1} \int d\nu(\lambda) [f_0(\lambda)]^{1-s} [f_1(\lambda)]^s. \quad (\text{D6})$$

The error exponent $-\ln P_{e,\min}$ approaches the Chernoff exponent ξ in an asymptotic sense [48].

For any POVM \mathcal{E} , a quantum lower bound on B is [28]

$$B \geq F \equiv \text{tr} \sqrt{\sqrt{\rho_0} \rho_1 \sqrt{\rho_0}}, \quad (\text{D7})$$

where F is the Uhlmann fidelity, while a quantum upper bound on ξ is [36]

$$\xi \leq \zeta \equiv -\ln \inf_{0 \leq s \leq 1} \text{tr}(\rho_0^{1-s} \rho_1^s). \quad (\text{D8})$$

[1] M. Tsang, R. Nair, and X.-M. Lu, Quantum Theory of Super-resolution for Two Incoherent Optical Point Sources, *Phys. Rev. X* **6**, 031033 (2016).
 [2] M. Tsang, Resolving starlight: A quantum perspective, *Contemp. Phys.* **60**, 279 (2019).
 [3] M. Tsang and R. Nair, Fundamental quantum limits to wave-form detection, *Phys. Rev. A* **86**, 042115 (2012).
 [4] S. Ng, S. Z. Ang, T. A. Wheatley, H. Yonezawa, A. Furusawa, E. H. Huntington, and M. Tsang, Spectrum analysis

with quantum dynamical systems, *Phys. Rev. A* **93**, 042121 (2016).
 [5] D. Budker and M. Romalis, Optical magnetometry, *Nat. Phys.* **3**, 227 (2007).
 [6] K. M. Backes, D. A. Palken, S. A. Kenany, B. M. Brubaker, S. B. Cahn, A. Droster, G. C. Hilton, S. Ghosh, H. Jackson, S. K. Lamoreaux, A. F. Leder, K. W. Lehnert, S. M. Lewis, M. Malnou, R. H. Maruyama, N. M. Rapidis, M. Simanovskaia, S. Singh, D. H. Speller, I. Urdinaran *et al.*, A quantum

- enhanced search for dark matter axions, *Nature (London)* **590**, 238 (2021).
- [7] A. S. Holevo, *Probabilistic and Statistical Aspects of Quantum Theory* (Scuola Normale Superiore Pisa, Pisa, 2011).
- [8] C. W. Helstrom, *Quantum Detection and Estimation Theory* (Academic, New York, 1976).
- [9] X.-M. Lu, H. Krovi, R. Nair, S. Guha, and J. H. Shapiro, Quantum-optimal detection of one-versus-two incoherent optical sources with arbitrary separation, *npj Quantum Inf.* **4**, 64 (2018).
- [10] M. Tsang, Subdiffraction incoherent optical imaging via spatial-mode demultiplexing, *New J. Phys.* **19**, 023054 (2017).
- [11] Z. Dutton, R. Kerviche, A. Ashok, and S. Guha, Attaining the quantum limit of superresolution in imaging an object's length via predetection spatial-mode sorting, *Phys. Rev. A* **99**, 033847 (2019).
- [12] M. Tsang, Subdiffraction incoherent optical imaging via spatial-mode demultiplexing: Semiclassical treatment, *Phys. Rev. A* **97**, 023830 (2018).
- [13] M. Tsang, Quantum limit to subdiffraction incoherent optical imaging, *Phys. Rev. A* **99**, 012305 (2019).
- [14] S. Zhou and L. Jiang, Modern description of Rayleigh's criterion, *Phys. Rev. A* **99**, 013808 (2019).
- [15] M. Tsang, Semiparametric estimation for incoherent optical imaging, *Phys. Rev. Res.* **1**, 033006 (2019).
- [16] M. Tsang, Quantum limit to subdiffraction incoherent optical imaging. II. A parametric-submodel approach, *Phys. Rev. A* **104**, 052411 (2021).
- [17] M. Tsang, Efficient superoscillation measurement for incoherent optical imaging, *IEEE J. Sel. Top. Signal Process.* (2022), doi: 10.1109/JSTSP.2022.3212173.
- [18] M. Tsang, Quantum metrology with open dynamical systems, *New J. Phys.* **15**, 073005 (2013).
- [19] M. Tsang, H. M. Wiseman, and C. M. Caves, Fundamental Quantum Limit to Waveform Estimation, *Phys. Rev. Lett.* **106**, 090401 (2011).
- [20] M. A. Nielsen and I. L. Chuang, *Quantum Computation and Quantum Information* (Cambridge University Press, Cambridge, 2011).
- [21] M. Aspelmeyer, T. J. Kippenberg, and F. Marquardt, Cavity optomechanics, *Rev. Mod. Phys.* **86**, 1391 (2014).
- [22] S. Nimmrichter, K. Hornberger, and K. Hammerer, Optomechanical Sensing of Spontaneous Wave-Function Collapse, *Phys. Rev. Lett.* **113**, 020405 (2014).
- [23] N. Christensen, Stochastic gravitational wave backgrounds, *Rep. Prog. Phys.* **82**, 016903 (2019).
- [24] C. W. Gardiner and P. Zoller, *Quantum Noise*, 2nd ed. (Springer, Berlin, 2000).
- [25] J. H. Shapiro, The quantum theory of optical communications, *IEEE J. Sel. Top. Quantum Electron.* **15**, 1547 (2009).
- [26] H. L. Van Trees, *Detection, Estimation, and Modulation Theory, Part I* (Wiley, New York, 2001).
- [27] R. H. Shumway and D. S. Stoffer, *Time Series Analysis and Its Applications* (Springer, Cham, 2017).
- [28] M. Hayashi, *Quantum Information Theory: Mathematical Foundation*, 2nd ed. (Springer, Berlin, 2017).
- [29] S. Alipour and A. T. Rezakhani, Extended convexity of quantum Fisher information in quantum metrology, *Phys. Rev. A* **91**, 042104 (2015).
- [30] J. Řeháček, M. Paúr, B. Stoklasa, Z. Hradil, and L. L. Sánchez-Soto, Optimal measurements for resolution beyond the Rayleigh limit, *Opt. Lett.* **42**, 231 (2017).
- [31] C. M. Caves, Quantum-mechanical noise in an interferometer, *Phys. Rev. D* **23**, 1693 (1981).
- [32] H. J. Kimble, Y. Levin, A. B. Matsko, K. S. Thorne, and S. P. Vyatchanin, Conversion of conventional gravitational-wave interferometers into quantum nondemolition interferometers by modifying their input and/or output optics, *Phys. Rev. D* **65**, 022002 (2001).
- [33] M. Tsang and C. M. Caves, Coherent Quantum-Noise Cancellation for Optomechanical Sensors, *Phys. Rev. Lett.* **105**, 123601 (2010).
- [34] J. H. Shapiro, Quantum measurement eigenkets for continuous-time direct detection, *Quantum Semiclass. Opt. B* **10**, 567 (1998).
- [35] P. Whittle, The analysis of multiple stationary time series, *J. R. Stat. Soc. B* **15**, 125 (1953).
- [36] K. M. R. Audenaert, M. Nussbaum, A. Szkoła, and F. Verstraete, Asymptotic error rates in quantum hypothesis testing, *Commun. Math. Phys.* **279**, 251 (2008).
- [37] Z. Huang and C. Lupo, Quantum Hypothesis Testing for Exoplanet Detection, *Phys. Rev. Lett.* **127**, 130502 (2021).
- [38] U. Zanforlin, C. Lupo, P. W. R. Connolly, P. Kok, G. S. Buller, and Z. Huang, Optical quantum super-resolution imaging and hypothesis testing, *Nat. Commun.* **13**, 5373 (2022).
- [39] S. L. Danilishin, F. Y. Khalili, and H. Miao, Advanced quantum techniques for future gravitational-wave detectors, *Living Rev. Relativ.* **22**, 2 (2019).
- [40] M. Tse *et al.*, Quantum-Enhanced Advanced LIGO Detectors in the Era of Gravitational-Wave Astronomy, *Phys. Rev. Lett.* **123**, 231107 (2019).
- [41] T. Gefen, A. Rotem, and A. Retzker, Overcoming resolution limits with quantum sensing, *Nat. Commun.* **10**, 4992 (2019).
- [42] S. L. Mouradian, N. Glikin, E. Megidish, K.-I. Eilers, and H. Haeflner, Quantum sensing of intermittent stochastic signals, *Phys. Rev. A* **103**, 032419 (2021).
- [43] W. Górecki, A. Riccardi, and L. Maccone, Quantum Metrology of Noisy Spreading Channels, *Phys. Rev. Lett.* **129**, 240503 (2022).
- [44] H. Shi and Q. Zhuang, Ultimate precision limit of noise sensing and dark matter search, *arXiv:2208.13712*.
- [45] M. Tsang, F. Albarelli, and A. Datta, Quantum Semiparametric Estimation, *Phys. Rev. X* **10**, 031023 (2020).
- [46] J. A. Gross and C. M. Caves, One from many: Estimating a function of many parameters, *J. Phys. A: Math. Theor.* **54**, 014001 (2021).
- [47] T. Kailath, The divergence and Bhattacharyya distance measures in signal selection, *IEEE Trans. Commun. Technol.* **15**, 52 (1967).
- [48] B. C. Levy, *Principles of Signal Detection and Parameter Estimation* (Springer, New York, 2008).